Top squarks from the landscape at high luminosity LHC

Howard Baer,[1,*] Vernon Barger,[2,†] Juhi Dutta,[1,‡] Dibyashree Sengupta,[3,‖] and Kairui Zhang[2,§]

[1]*Homer L. Dodge Department of Physics and Astronomy, University of Oklahoma, Norman, Oklahoma 73019, USA*

[2]*Department of Physics, University of Wisconsin, Madison, Wisconsin 53706, USA*

[3]*INFN, Laboratori Nazionali di Frascati, Via E. Fermi 54, 00044 Frascati (RM), Italy*

(Received 23 July 2023; accepted 3 October 2023; published 27 October 2023)

Supersymmetric models with low electroweak fine-tuning are expected to be more prevalent on the string landscape than fine-tuned models. We assume a fertile patch of landscape vacua containing the minimal supersymmetric standard model as low energy/weak scale effective field theory. Then, a statistical pull by the landscape to large soft terms is balanced by the requirement of a derived value of the weak scale which is not too far from its measured value in our Universe. Such models are characterized by light Higgsinos in the few hundred GeV range whilst top squarks are in the 1–2.5 TeV range with large trilinear soft terms which helps to push $m_h \sim 125$ GeV. Other sparticles are generally beyond current LHC reach and the BR$(b \to s\gamma)$ branching fraction is nearly equal to its standard model value. The light top-squarks decay comparably via $\tilde{t}_1 \to b\tilde{\chi}_1^+$ and $\tilde{t}_1 \to t\tilde{\chi}_{1,2}^0$ yielding mixed final states of $b\bar{b} + \not{E}_T$, $t\bar{b}/\bar{t}b + \not{E}_T$, and $t\bar{t} + \not{E}_T$. We evaluate prospects for top squark discovery at high-luminosity LHC for the well-motivated case of natural SUSY from the landscape. We find for high luminosity LHC a 5σ reach out to $m_{\tilde{t}_1} \sim 1.65$ TeV and a 95% CL exclusion reach to $m_{\tilde{t}_1} \sim 1.95$ TeV. These reaches cover most (but not all) of the allowed stringy natural parameter space.

DOI: 10.1103/PhysRevD.108.075027

I. INTRODUCTION

The lightest supersymmetric (SUSY) partner of the top quark, the so-called top-squark $\tilde{t}_1$, has for long been a lucrative target for supersymmetry searches at hadron colliders. Early estimates of Ellis, Enqvist, Nanopoulos and Zwirner/background (BG) [1,2] naturalness, using the measure $\Delta_{\rm BG} \equiv \max_i |\frac{p_i}{m_Z^2}\frac{\partial m_Z^2}{\partial p_i}| < \Delta_{\rm BG}(\max)$ (where the p_i are taken as fundamental theory parameters, usually assumed to be a set of high scale soft SUSY breaking terms) found $m_{\tilde{t}_1} \lesssim 300$–$400$ GeV for $\Delta_{\rm BG} < 10$–30 [3]. Using an alternative measure $\delta m_h^2/m_h^2 < \Delta_{\rm HS}$, it was expected that three third generation squarks should all have mass $m_{\tilde{t}_{1,2},\tilde{b}_1} \lesssim 500$ GeV [4–6]. These theoretical naturalness computations may be compared to recent limits from LHC searches where both ATLAS [7,8] and CMS [9] find that $m_{\tilde{t}_1} \gtrsim 1.2$ TeV from pp collisions at $\sqrt{s} = 13$ TeV and with ~139 fb^{-1} of integrated luminosity.[1] Taken at face value, this confrontation between theory and experiment would indicate that the paradigm of weak scale supersymmetry [10] is highly implausible as a route to physics beyond the Standard Model (SM) [11].

One resolution to the supersymmetry naturalness conflict is that the early theoretical naturalness calculations turned out to be large overestimates of the actual fine-tuning [12,13]. For the BG measure, it is emphasized in Refs. [12–15] that the fundamental theory parameters p_i should not be taken as a set of independent soft SUSY breaking terms, since in any more UV-complete theory, these are all correlated. For example, in gravity-mediation SUSY breaking models with a well-specified SUSY

*baer@ou.edu
†barger@pheno.wisc.edu
‡juhi.dutta@ou.edu
‖Dibyashree.Sengupta@lnf.infn.it
§kzhang89@wisc.edu

[1]The ATLAS and CMS experiments have published several different recent limits for different assumed simplified models [7–9]. The references quoted here assume stop pair production followed by 100% decay $\tilde{t}_1 \to t\tilde{\chi}_1^0$, but with different assumptions for the $t \to bW$ final state (hadronic or leptonic). The 95% CL exclusion limits from simplified models hover around $m_{\tilde{t}_1} \gtrsim 1.1$–$1.3$ TeV. In the following plots, we will adopt $m_{\tilde{t}_1} \gtrsim 1.2$ TeV and mark the limit by a wiggly line to denote its inherent uncertainty.

breaking sector, then the soft terms are all computed as multiples of the gravitino mass $m_{3/2}$.[2] Adopting independent soft terms as the p_i just parametrizes our ignorance of the SUSY breaking mechanism, but can lead to overestimates of finetuning by up to three orders of magnitude [13]. Alternatively, the $\Delta_{\rm HS}$ measure attempts to tune dependent quantities $m_{H_u}^2$ and $\delta m_{H_u}^2$ one against the other, which again leads to up to three orders of magnitude overestimates of fine-tuning [13]. If one instead adopts the more conservative electroweak fine-tuning measure $\Delta_{\rm EW}$ [17,18], then top-squark masses are allowed up to several TeV at little cost to fine-tuning since their contributions to the weak scale are suppressed by loop factors (for a recent review, see, e.g., Ref. [19]).

In most supersymmetric models of particle physics—even in the case of high scale scalar mass universality—the lighter top squark $\tilde{t}_1$ is expected to be the lightest of all the squarks. It thus presents a lucrative target for supersymmetry discovery at hadron collider experiments such as the CERN LHC. The lightness of the top squark, relative to other squarks, arises from two reasons: 1. the large top-quark Yukawa coupling f_t acts to drive top squark soft terms to lower values than other squarks (assuming an initial degeneracy amongst all squark soft terms at the high scale) and 2. the large top Yukawa enhances the mixings amongst the top squarks, and large mixing typically acts to further split the top squark eigenmasses, driving the lighter one down and the heavier stop $\tilde{t}_2$ to larger values (relative to the no mixing case).

A third effect arises from the string landscape picture [20–22]. In the string landscape, where of order 10^{500} vacua solutions [23] arise from compactification from 10 to 4 spacetime dimensions, then each vacuum solution corresponds to a different set of $4-d$ low energy effective field theory law of physics. The string landscape provides a natural setting for Weinberg's anthropic solution to the cosmological constant problem [24] in an eternally inflating multiverse. If similar reasoning is applied to the origin of the SUSY breaking scale, then it is expected that no particular value of the (complex-valued) SUSY breaking F terms or (real-valued) SUSY breaking D terms are favored over any other. In that case, then on rather general grounds, the landscape is expected to statistically favor large soft terms via a power law [25]

$$f_{\rm SUSY} \sim m_{\rm soft}^{2n_F+n_D-1}, \tag{1}$$

where $f_{\rm SUSY}$ encodes the expected statistical distribution of landscape soft terms. Thus, even the textbook case of SUSY breaking via a single F-term field would yield a linear draw to large soft terms.

Naively, one might expect such a distribution to favor high scale SUSY breaking. However, the weak scale soft terms and SUSY-preserving μ parameter determine the magnitude of the weak scale via the scalar potential minimization conditions under the radiative breaking of electroweak symmetry:

$$m_Z^{\rm PU2} = \frac{m_{H_d}^2 + \Sigma_d^d - (m_{H_u}^2 + \Sigma_u^u)\tan^2\beta}{\tan^2\beta - 1} - \mu_{\rm PU}^2 \tag{2}$$

where the label PU stands for parameter values in each separate pocket universe within the greater multiverse. Here, following Weinberg, we assume a so-called fertile patch of the multiverse wherein the low energy/weak scale effective field theory consists of the minimal supersymmetric SM (MSSM) (plus some additional fields such as a Peccei-Quinn (PQ) sector) but with variable soft terms and hence variable values for the associated weak scale $m_{\rm weak}^{\rm PU}$. The value of $m_{\rm weak}^{\rm PU}$ is typically $\neq m_{\rm weak}^{\rm OU}$, where OU stands for a quantity's value in our Universe. Agrawal *et al.* (ABDS) [26] have shown that for complex nuclei—and hence atoms as we know them—to form in a PU, that the value of $m_{\rm weak}^{\rm PU}$ must lie within the ABDS window, typically $m_{\rm weak}^{\rm PU} \sim (0.5-5)m_{\rm weak}^{\rm OU}$ (the atomic principle). The ABDS anthropic window thus vetoes vacua with improper electroweak symmetry breaking (EWSB), such as solutions with no EWSB or charge or color breaking (CCB) minima; it also excludes the vast majority of high scale SUSY solutions that typically lead to $m_{\rm weak}^{\rm PU}$ far beyond the ABDS window. The string landscape approach to soft SUSY breaking within the MSSM has led to some success in that it statistically predicts a Higgs boson mass $m_h \simeq 125$ GeV whilst sparticles are typically well beyond current LHC search bounds [27].

Returning to top squarks, the large value of the top quark Yukawa coupling enhances the radiative correction terms $\Sigma_u^u(\tilde{t}_{1,2})$ in Eq. (2) relative to $\Sigma_u^u(\tilde{q}_i)$ (where $\tilde{q}_i$ denotes squark masses of the first two generations). Thus, for independent soft terms for each generation (as is generic in gravity mediation [16,28,29]) then the squark and slepton masses of the first two generations will get pulled to much higher values, typically $m_{\tilde{q}_i} \sim 10$–40 TeV (providing a mixed decoupling/quasidegeneracy solution to the SUSY flavor and CP problems [30]) whilst $m_{\tilde{t}_1} \sim 1$–2.5 TeV. As such, the string landscape provides additional strong motivation for top-squark pair searches at LHC as compared to other sparticle searches (although the search for light Higgsinos with $m(\text{Higgsino}) \sim 100$–$400$ GeV is also especially lucrative [31–36]).

In this paper, after a brief review of some previous relevant works in Sec. I A, in Sec. II we will present landscape predictions for some of the relevant properties of light top squarks as derived from string landscape predictions with a simple $n=1$ power law draw to large soft terms. We will find that while large stop mixing terms $m_t A_t$ are expected at the weak scale (and indeed these help boost up the light Higgs mass to $m_h \sim 125$ GeV), the lighter top squark $\tilde{t}_1$ is still typically mainly a right-top squark [assuming high scale

[2]For instance, in dilaton-dominated SUSY breaking, then $m_0 = m_{3/2}$ with $A_0 = -m_{1/2} = \sqrt{3}m_{3/2}$ [16].

degeneracy of left and right top squark soft terms $m_{\tilde{t}_L}$ and $m_{\tilde{t}_R}$, as expected by intragenerational degeneracy since the elements of each generation fill out the 16-dimensional spinor-rep of $SO(10)$]. Also, we will find that the branching fraction $\mathrm{BR}(b \to s\gamma)$ is expected to be very near its SM value (in agreement with data and in accord with the general expectation for TeV-scale top squarks). We will also determine the expected $\tilde{t}_1$ branching fractions which will determine the associated LHC search signatures. In Sec. III, we examine top-squark pair production rates and expected signal channels which are expected for high-luminosity LHC (HL-LHC) searches. In Sec. IV we introduce a natural top-squark benchmark point and associated model line. In Sec. V, we give cuts and m_{T2} distributions for each of the three major signal channels. By combining results, we present 5σ reach and 95% CL exclusion limits versus $m_{\tilde{t}_1}$. In Sec. VI, we present a brief summary and conclusions from our results.

A. A brief review of some previous relevant works

The first few papers on top-squark phenomenology focused on the possibility for $t \to \tilde{t}_1\tilde{\chi}_i^0$ decays which could disrupt top-quark discovery signatures at the CERN $Sp\bar{p}S$ [37,38] and Fermilab Tevatron colliders [39]. Direct top-squark pair production at the Tevatron within the framework of simplified models was already examined in Ref. [40] shortly before the actual discovery of the top-quark. In Ref. [41], the capability of LHC to measure the top-quark mixing angle θ_t was examined: the strategy promoted was to as best as one can measure the various top-squark branching fractions into different decay modes which depend on stop mixing. In Ref. [42], the scenario of maximal stop mixing, which provides an explanation for the rather high Higgs mass $m_h \simeq 125$ GeV, was examined with a view towards resolving the apparent tension between naturalness and the light Higgs mass. In Ref. [43], Graesser and Shelton examined top squark pair production followed by mixed top-squark decay modes $\tilde{t}_1 \to b\tilde{\chi}_1^+$ with $\tilde{t}_1^* \to \bar{t}\tilde{\chi}_1^0$ and suggested a new search variable $t =$ topness to aid in identifying top jets in the final state. In Ref. [44], it is argued that conventional fine-tuning measures overestimated the severeness of top-squark mass upper bounds and instead examined implications of the Δ_{EW} measure for top-squark properties. Using $\Delta_{\mathrm{EW}} \lesssim 30$, then top squarks may range up to $m_{\tilde{t}_1} \lesssim 3$ TeV provided there is a rather large weak scale A_t soft term mixing value which also elevates the Higgs mass $m_h \to \sim 125$ GeV. Thus, there exists a significant portion of natural SUSY parameter space that lies beyond ATLAS/CMS limits as displayed in the $m_{\tilde{t}_1}$ vs $m_{\tilde{\chi}_1^0}$ simplified model parameter plane. In C. Han *et al.* [45], the authors recast various ATLAS/CMS top squark search results into the $m_{\tilde{t}_1}$ vs $m_{\tilde{\chi}_1^0}$ top-squark search plane and compare against naturalness using Δ_{EW}. In Ref. [46], assuming $\tilde{t}_1 \to t\tilde{\chi}_1^0$ decay, Bai *et al.* impose a very strong $\not{E}_T$ cut against which two top jets merge. Cuts on the resulting configuration boost signal over background by 40% over conventional analyses.

In Ref. [47], the ATLAS collaboration examined the reach of HL-LHC for top-squark pair production followed by $\tilde{t}_1 \to t\tilde{\chi}_1^0$ in the top-squark search plane: for light $m_{\tilde{\chi}_1^0}$, they find using LHC14 with 3000 fb^{-1} a 5σ reach to $m_{\tilde{t}_1} \sim 1.25$ TeV and a 95% CL exclusion to $m_{\tilde{t}_1} \sim 1.7$ TeV. Similar results from CMS are shown in Ref. [48].

II. PROPERTIES OF TOP SQUARKS FROM THE LANDSCAPE

A. Scan over landscape

In this section, we wish to explore the predictions from the string landscape for top squark properties. To this end, we will generate the distribution

$$dN_{\mathrm{vac}} = f_{\mathrm{SUSY}} \cdot f_{\mathrm{EWSB}} \cdot f_{cc} \cdot dm_{\mathrm{soft}}, \tag{3}$$

where $dN_{\mathrm{vac}}/dm_{\mathrm{soft}}$ stands for the distribution of string vacua with respect to the soft SUSY breaking parameters. We will assume a fertile patch of the string landscape where the low energy/weak scale effective field theory consists of the MSSM (possibly augmented with a PQ sector that is only relevant for dark matter considerations), but where in the string landscape the various soft terms

$$m_0(1,2), m_0(3), m_{1/2}, A_0, \tan\beta, m_A, \mu \tag{4}$$

will scan independently [49]. (Note that while the soft terms would all be correlated and hence dependent in our Universe, as discussed earlier, they should scan independently within the various pocket universes within the greater multiverse.) The various independent soft terms scan as a power law

$$f_{\mathrm{SUSY}} \sim m_{\mathrm{soft}}^{2n_F+n_D-1}, \tag{5}$$

where n_F is the number of hidden sector F-breaking fields (distributed as complex numbers) and n_D is the number of D-breaking fields (distributed as real numbers). For simplicity, we will adopt the textbook case $n_F = 1$, a single F breaking field, and $n_D = 0$ so that $f_{\mathrm{SUSY}} \sim m_{\mathrm{soft}}^1$, i.e., a linear statistical draw to large soft terms. We will take the nonsoft term $\tan\beta$ to scan uniformly and will fix the μ parameter to a natural value $\mu = 200$ GeV. The cosmological constant selection embedded in f_{cc} does not impact the soft term selection as emphasized by Douglas [25].

For the (anthropic) selection f_{EWSB}, we require the derived value of the weak scale in each pocket universe to have 1. no charge or color breaking minima (no CCB), 2. an appropriate breakdown of EW symmetry to $U(1)_{\mathrm{EM}}$, and 3. a derived value for the pocket universe lies within the ABDS window [26], i.e., that $m_{\mathrm{weak}}^{\mathrm{PU}} \lesssim (0.5-5)m_{\mathrm{weak}}^{\mathrm{OU}}$. To be precise, in a pocket universe with no fine-tuning, this corresponds to $\Delta_{\mathrm{EW}} \lesssim 30$ since $m_{\mathrm{weak}}^{PU} \sim m_Z\sqrt{\Delta_{\mathrm{EW}}/2}$.

By combining the various effects in Eq. (3), we are able to obtain a measure of what Douglas calls stringy naturalness [50,51]. While stringy naturalness is not measured by a number, we can measure it via a scan over SUSY model soft terms in accord with Eq. (3). Here, we implement the $n \equiv 2n_F + n_D - 1 = 1$ linear scan over the NUHM3 [52] parameter space:

(1) $m_0(1,2)$:0.1–45 TeV,
(2) $m_0(3)$:0.1–10 TeV,
(3) $m_{1/2}$: 0.5–3 TeV,
(4) A_0: $0-(-20)$ TeV,
(5) $\tan\beta$:$3-60$ (uniform scan),
(6) m_A: 0.3–10 TeV,

with μ fixed at a natural value of 200 GeV.[3] For each set of input parameters in the NUHM3 model, we use Isajet 7.88 [54] to compute the corresponding sparticle and Higgs boson masses and other properties.

B. Top squark mass and mixing

Next, we wish to display properties of top squarks from probability distributions reflecting stringy naturalness. After our landscape scan, we display in Fig. 1 histograms of probability (a) dP/dm_h and (b) $dP/dm_{\tilde{t}_1}$. From frame (a), we see that the stringy naturalness prefers a light Higgs boson h with mass between 120 GeV $< m_h <$ 126 GeV with a peak at $m_h \sim 125$ GeV. This behavior arises due to maximizing the soft terms that enter into the radiatively corrected Higgs mass

$$m_h^2 \simeq m_Z^2 \cos^2 2\beta + \frac{3g^2}{8\pi^2}\frac{m_t^4}{m_W^2}\left[\ln\frac{m_{\tilde{t}}^2}{m_t^2} + \frac{x_t^2}{m_{\tilde{t}}^2}\left(1 - \frac{x_t^2}{12m_{\tilde{t}}^2}\right)\right], \tag{6}$$

where $x_t = A_t - \mu\cot\beta$ and $m_{\tilde{t}}^2 = m_{Q_3}m_{U_3}$ is an effective stop mass which minimizes log corrections to the scalar potential (here, m_{Q_3} and m_{U_3} are the third generation doublet and up-squark soft terms and A_t is the weak scale top-squark trilinear soft term). For a given value of $m_{\tilde{t}}^2$, this expression gives a maximal value for m_h when $x_t^{\max} = \sqrt{6}m_{\tilde{t}}$ [55–57]. The pull on the A_0 term to large values (but not so large as to enter CCB minima in the scalar potential) helps pull m_h up into the ~125 GeV range.

In frame (b), we show the probability distribution for $m_{\tilde{t}_1}$ from the string landscape with an $n = 1$ draw to large soft terms. While there is just a small probability to have a top squark with mass below a TeV, the distribution rises to a peak at $m_{\tilde{t}_1} \sim 1.5$ TeV followed by a slow dropoff ending around $m_{\tilde{t}_1} \sim 2.5$ TeV. We also show the present $m_{\tilde{t}_1} \gtrsim 1.2$ TeV limit from ATLAS/CMS searches (as a wiggly line to denote the inherent uncertainty associated with simplified model limits). By comparing, we see that LHC experiments are only beginning to probe the range of top squark masses predicted by the landscape. The reach of LHC run 3 and HL-LHC should push into the peak probability region in the coming years, making the search for light top squarks of supersymmetry a highly motivated priority.

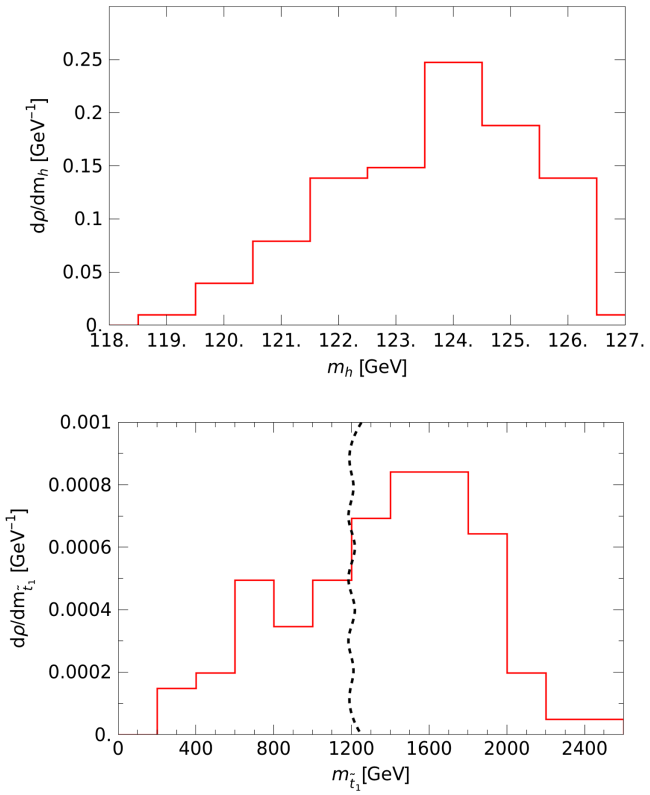

FIG. 1. (a) Probability distribution for light Higgs mass m_h. (b) Probability distribution for lighter top squark mass $m_{\tilde{t}_1}$. We assume statistical selection of soft terms from the string landscape with an $n = 1$ power-law draw to large soft terms.

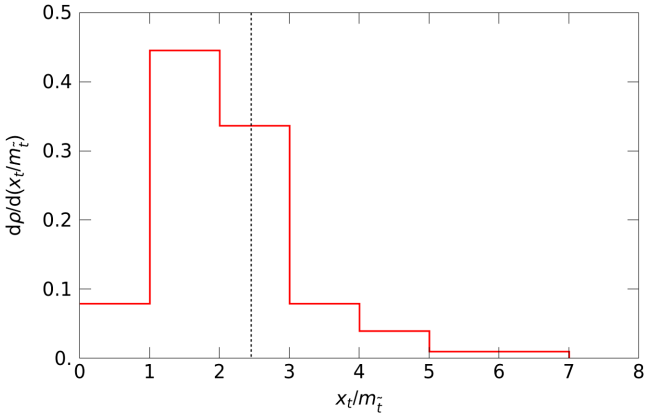

FIG. 2. Probability distribution $dP/d(x_t/m_{\tilde{t}})$. The vertical dashed line denotes where $x_t = \sqrt{6}m_{\tilde{t}}$ where the Higgs mass radiative corrections becomes maximal. We assume statistical selection of soft terms from the string landscape with an $n = 1$ power-law draw to large soft terms.

[3]The SUSY conserving μ parameter arises from whatever solution to the SUSY μ problem is imposed. For a review of 20 solutions to the SUSY μ problem, see Ref. [53].

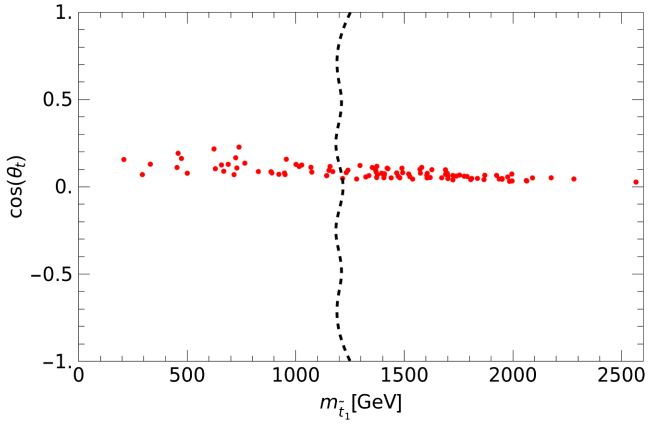

FIG. 3. Probability distribution for lighter top squark mass vs $\cos\theta_t$ where $\tilde{t}_1 = \cos\theta_t \tilde{t}_L - \sin\theta_t \tilde{t}_R$. We assume statistical selection of soft terms from the string landscape with an $n = 1$ power-law draw to large soft terms.

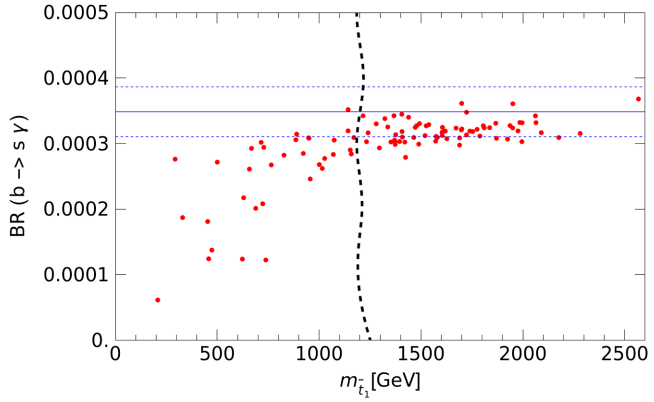

FIG. 4. Probability distribution for lighter top squark mass vs $\mathrm{BR}(b \to s\gamma)$. We assume statistical selection of soft terms from the string landscape with an $n = 1$ power-law draw to large soft terms. The horizontal lines show the PDG measured value $\pm 2\sigma$ error band while the vertical dashed line shows the approximate LHC limit on $m_{\tilde{t}_1}$ from simplified model analyses.

In Fig. 2, we show the differential probability distribution $dP/d(x_t/m_{\tilde{t}})$, where $m_{\tilde{t}} \equiv \sqrt{m_{\tilde{t}_1} m_{\tilde{t}_2}}$. The vertical dashed line denotes where $x_t = \sqrt{6} m_{\tilde{t}}$, which is where the radiative corrections to the Higgs mass from top squarks are maximal. The distribution peaks just below this point due to the landscape selection of large trilinear soft terms A_t. This draw to large A_t, and hence large x_t, helps to understand why the Higgs mass m_h is pushed up to $m_h \sim 125$ GeV in the string landscape.

In Fig. 3, we plot dots of stringy naturalness in the $m_{\tilde{t}_1}$ vs $\cos\theta_t$ plane where the light top squark

$$\tilde{t}_1 = \cot\theta_t \tilde{t}_L - \sin\theta_t \tilde{t}_R \tag{7}$$

in the notation of Ref. [10], and where θ_t is the top squark mixing angle and $\tilde{t}_L$ and $\tilde{t}_R$ are the weak scale left- and right-stop eigenstates. From the plot, we see that $\cos\theta_t \sim 0.1$ over the entire expected range of light top squark masses so that we expect the light top-squark to be predominantly of $\tilde{t}_R$ variety in spite of the expected large stop mixing. This is because, starting with common soft top-squark masses at the high scale $m_{Q_3} = m_{U_3} = m_{D_3} \equiv m_0(3)$, the renormalization group evolution suppresses the right top-squark soft mass m_{U_3} more than the left top squark soft mass m_{Q_3}.

1. $b \to s\gamma$ branching fraction

A powerful virtual probe of top squark properties comes from the measured value of the flavor-changing b decay branching fraction $\mathrm{BR}(b \to s\gamma)$. In the SM, this process proceeds via a tW loop while in two-Higgs doublet models there is a comparable contribution from a $tH^{\pm}$ loop [58]. In the MSSM, there are additional contributions from $\tilde{t}_i \tilde{\chi}^{\pm}_{1,2}$ and even $\tilde{q}\tilde{\chi}^{\pm}_{1,2}$ loops (the latter tend to decouple in our picture since first/second generation squarks are drawn to $m_{\tilde{q}_i} \sim 10$–40 TeV level (since their contributions to the weak scale are suppressed by their tiny Yukawa couplings).

For top-squark and chargino masses nearby to the weak scale, then the various stop loops tend to dominate the contributions to the C_7 Wilson coefficient albeit with either positive or negative contributions [59]. Nonetheless, one expects with rather light top-squarks of a few hundred GeV that there would be large measured deviations in the $\mathrm{BR}(b \to s\gamma)$ compared to its SM value. For top squarks approaching the TeV scale, then these contributions decouple and one expects the SUSY value for $\mathrm{BR}(b \to s\gamma)$ to nearly match the SM expectation. For our theory calculation, we adopt the next-to-leading-order (NLO) evaluation which is included in Isajet [59,60]. The Isajet value, which does not include two-loop and nonperturbative effects, asymptotes to $\mathrm{BR}(b \to s\gamma)^{\mathrm{Isajet}}_{\mathrm{SM}} \sim 3.15 \times 10^{-4}$. Thus, along with the Isajet NLO perturbative estimate, we include a two-loop and nonperturbative contribution $\delta\Gamma \equiv \delta\Gamma_{2\text{-loop}} + \delta\Gamma_{\mathrm{nonp}} \simeq 0.25$ as emphasized by Misiak [61].

The present measured average value from the HFLAV Collaboration [62] is given as $\mathrm{BR}(b \to s\gamma) = (3.49 \pm 0.19) \times 10^{-4}$, which is dominated by the Belle [63] and *BABAR* [64] measurements. The current SM theory estimate is $\mathrm{BR}(b \to s\gamma)^{\mathrm{TH}}_{\mathrm{SM}} = (3.36 \pm 0.23) \times 10^{-4}$ [61].

In Fig. 4, we plot points of stringy naturalness in the $m_{\tilde{t}_1}$ vs $\mathrm{BR}(b \to s\gamma)$ plane. The blue solid line and dashed bands show the HFLAV value $\pm 2\sigma$. The theory values cluster around $\mathrm{BR}(b \to s\gamma) \sim 3.4 \times 10^{-4}$ with some larger deviations for lower $m_{\tilde{t}_1} \lesssim 1$ TeV. Thus, the measured $\mathrm{BR}(b \to s\gamma)$ branching fraction tends to support the scenario of TeV-scale top squarks as predicted by the string landscape and as expected from the rather large value of the light Higgs mass $m_h \sim 125$ GeV.

2. Top squark branching fractions

The top squark decay widths $\Gamma(\tilde{t}_1 \to t\tilde{\chi}^0_i)$ $(i = 1$–$4)$ and $\Gamma(\tilde{t}_1 \to b\tilde{\chi}^+_j)$ $(j = 1$–$2)$ are expected to be the dominant

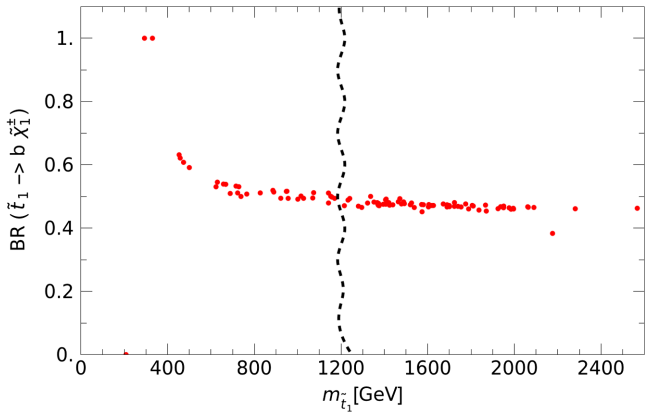

FIG. 5. Probability distribution for lighter top squark mass vs $\mathrm{BF}(\tilde{t}_1 \to b\tilde{\chi}_1^+)$. We assume statistical selection of soft terms from the string landscape with an $n = 1$ power-law draw to large soft terms.

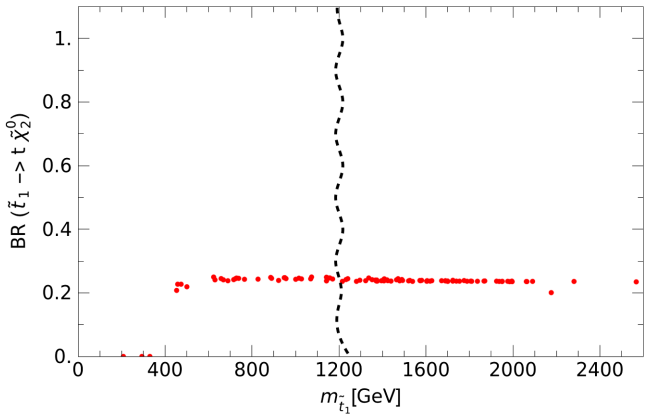

FIG. 7. Probability distribution for lighter top squark mass vs $\mathrm{BF}(\tilde{t}_1 \to t\tilde{\chi}_2^0)$. We assume statistical selection of soft terms from the string landscape with an $n = 1$ power-law draw to large soft terms.

top-squark decay modes and their formulas are listed in Ref. [10] as Eqs. (B.39) and (B.43), respectively. The numerical values can be extracted from the Isajet [54] code. The decay widths depend sensitively on the top-squark gauge couplings and the top-quark Yukawa coupling along with the mixing angle θ_t and the decay kinematics. In Fig. 5 we show the stringy natural values of $\mathrm{BF}(\tilde{t}_1 \to b\tilde{\chi}_1^+)$ vs $m_{\tilde{t}_1}$. From the plot, we see a rather uniform prediction vs $m_{\tilde{t}_1}$ that $\mathrm{BF}(\tilde{t}_1 \to b\tilde{\chi}_1^+)$ occurs very close to the 50% level.

In Fig. 6, we show the prediction for $\mathrm{BF}(\tilde{t}_1 \to t\tilde{\chi}_1^0)$ vs $m_{\tilde{t}_1}$. The result here is also rather uniform in $m_{\tilde{t}_1}$: that $\mathrm{BF}(\tilde{t}_1 \to t\tilde{\chi}_1^0) \sim 20$–$25\%$. Likewise, in Fig. 7 we show the $\mathrm{BF}(\tilde{t}_1 \to t\tilde{\chi}_2^0)$. This branching fraction also tends to occur at the 20–25% level with little variation vs $m_{\tilde{t}_1}$. Further branching fractions such as $\mathrm{BF}(\tilde{t}_1 \to t\tilde{\chi}_3^0)$ can occur at the several percent level, while others such as $\tilde{t}_1 \to t\tilde{\chi}_4^0$ and $\tilde{t}_1 \to b\tilde{\chi}_2^+$ tend to occur at the subpercent level.

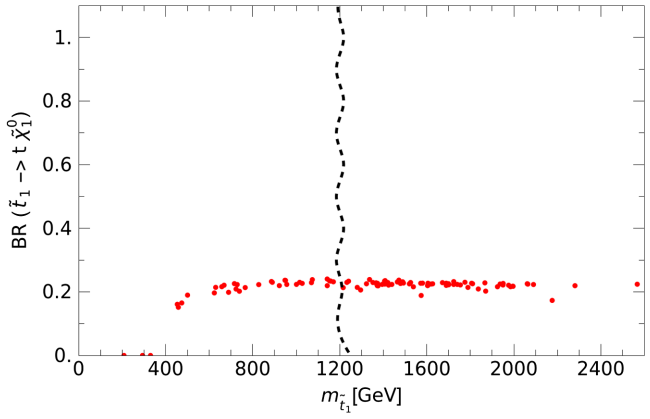

FIG. 6. Probability distribution for lighter top squark mass vs $\mathrm{BF}(\tilde{t}_1 \to t\tilde{\chi}_1^0)$. We assume statistical selection of soft terms from the string landscape with an $n = 1$ power-law draw to large soft terms.

III. PRODUCTION AND DECAY OF TOP SQUARKS AT LHC

For the benefit of the reader, we show in Fig. 8 the NLO Prospino [65] prediction for top squark pair production at LHC with $\sqrt{s} = 14$ TeV collisions: $\sigma(pp \to \tilde{t}_1\tilde{t}_1^* X)$ vs $m_{\tilde{t}_1}$. Starting just above the present LHC excluded region, with $m_{\tilde{t}_1} = 1.25$ TeV, we find $\sigma(\tilde{t}_1\tilde{t}_1^*) \sim 1$ fb, corresponding to 3000 signal events assuming the nominal HL-LHC integrated luminosity of 3 ab^{-1}. Even for $m_{\tilde{t}_1}$ as high as 2 TeV, we find $\sigma(\tilde{t}_1\tilde{t}_1^*) \sim 0.02$ fb, corresponding to 60 signal events at HL-LHC before cuts.

The projected HL-LHC reach for top squark pair production is usually presented in terms of simplified models by the ATLAS and CMS collaborations where a single top squark decay mode is assumed. We see from the previous subsection that such analyses are not realistic from the point of view of the string landscape and so we will

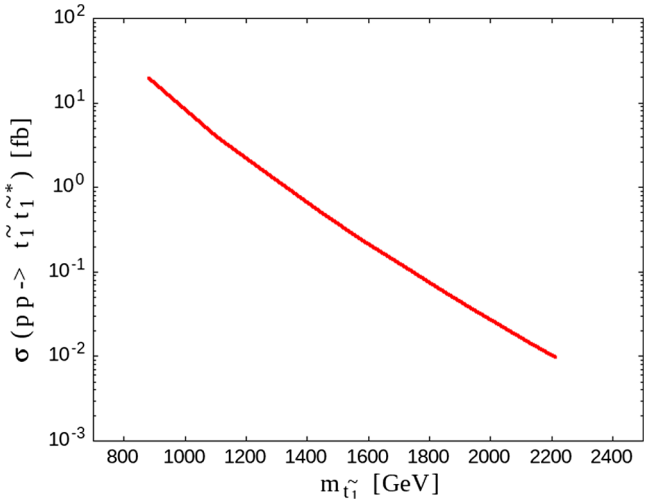

FIG. 8. Plot of $\sigma(pp \to \tilde{t}_1\tilde{t}_1^* X)$ from Prospino (NLO) versus $m_{\tilde{t}_1}$ for pp collisions at $\sqrt{s} = 14$ TeV.

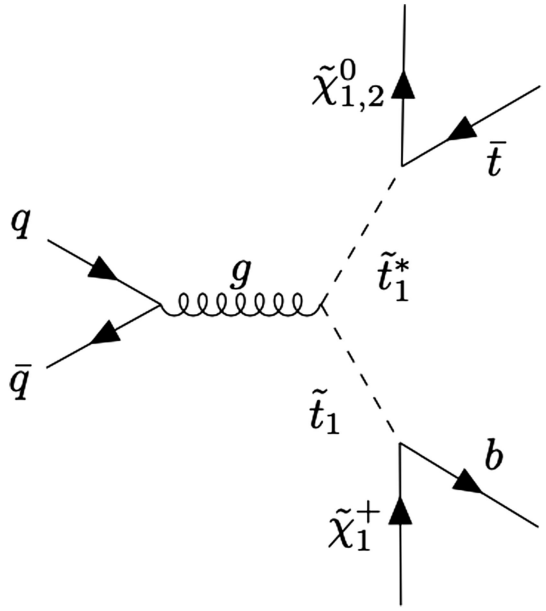

FIG. 9. Representative diagram for top squark pair production and decay at LHC in natural SUSY.

examine the reach of LHC at HL-LHC using the several predicted decay modes. This will give rise to mixed decay mode configurations such as is shown in Fig. 9 where one $\tilde{t}_1 \to b\tilde{\chi}^+_1$ and the other $\tilde{t}_1 \to t\tilde{\chi}^0_1$. Thus, we expect three main signal channels:

(1) $b\bar{b} + \not{E}_T$,
(2) $t\bar{t} + \not{E}_T$, and
(3) $t\bar{b} + \not{E}_T$ (plus charge conjugate mode).

In addition, some subset of events will contain soft decay products from the unstable Higgsinos in the cascade decay. Of particular note is the occasional presence of $\tilde{\chi}^0_2 \to \tilde{\chi}^0_1 \ell\overline{\ell}$ (with $\ell = e$ or μ), where $m(\ell\overline{\ell}) < m_{\tilde{\chi}^0_2} - m_{\tilde{\chi}^0_1}$.

IV. A STRINGY NATURAL TOP SQUARK BENCHMARK POINT

In the following section, we will examine top squark pair production at LHC14 for the following benchmark (BM) point, which is typical of stringy natural models. The BM point comes from the NUHM2 model [52] with parameters as listed in the Table I. It is a natural SUSY benchmark point since $\Delta_{\rm EW} = 22$, even though the lightest top squark lies at $m_{\tilde{t}_1} \sim 1.7$ TeV and $m_{\tilde{g}} \sim 2.8$ TeV. The BM point wino mass $M_2 \sim 1$ TeV, which is very close to recent exclusion limits from ATLAS [66] [for which $m(\text{wino}) \gtrsim$ 900 GeV from various simplified model analyses]. We have checked using the SModelS code [67,68] that our benchmark point is allowed by current LHC search results. Our benchmark model line is also allowed under LHC13 stop pair and EWino pair searches via the CheckMATE code [69,70]. Even so, the wino roughly decouples from lighter stop decays due to the fact that the light stop is mainly right stop (as seen from Fig. 3) and so hardly couples to winos. The stop decay to binos is suppressed by phase space and due to the smaller $U(1)_Y$ gauge coupling so stop decays to Higgsinos are dominant as shown in Figs. 5–7.

TABLE I. Input parameters (TeV) and masses (GeV) for the stringy natural SUSY benchmark point from the NUHM2 model with $m_t = 173.2$ GeV using Isajet 7.88 [54].

Parameter	Stringy natural BM point
m_0	5 TeV
$m_{1/2}$	1.2 TeV
A_0	−8 TeV
$\tan\beta$	10
μ	250 GeV
m_A	2 TeV
$m_{\tilde{g}}$	2830 GeV
$m_{\tilde{u}_L}$	5440 GeV
$m_{\tilde{u}_R}$	5561 GeV
$m_{\tilde{e}_R}$	4822 GeV
$m_{\tilde{t}_1}$	1714 GeV
$m_{\tilde{t}_2}$	3915 GeV
$m_{\tilde{b}_1}$	3949 GeV
$m_{\tilde{b}_2}$	5287 GeV
$m_{\tilde{\tau}_1}$	4746 GeV
$m_{\tilde{\tau}_2}$	5110 GeV
$m_{\tilde{\nu}_\tau}$	5107 GeV
$m_{\tilde{\chi}^\pm_1}$	261.7 GeV
$m_{\tilde{\chi}^\pm_2}$	1020.6 GeV
$m_{\tilde{\chi}^0_1}$	248.1 GeV
$m_{\tilde{\chi}^0_2}$	259.2 GeV
$m_{\tilde{\chi}^0_3}$	541.0 GeV
$m_{\tilde{\chi}^0_4}$	1033.9 GeV
m_h	124.7 GeV
$\Omega^{\rm std}_{\tilde{\chi}^0_1}h^2$	0.016
$\text{BR}(b \to s\gamma) \times 10^4$	3.1
$\text{BR}(B_s \to \mu^+\mu^-) \times 10^9$	3.8
$\sigma^{\rm SI}(\tilde{\chi}^0_1, p)$ (pb)	2.2×10^{-9}
$\sigma^{\rm SD}(\tilde{\chi}^0_1, p)$ (pb)	2.9×10^{-5}
$\langle\sigma v\rangle\|_{v\to 0}$ (cm^3/ sec)	1.3×10^{-25}
$\Delta_{\rm EW}$	22

The spectra is generated using the Isasugra code [71] from Isajet [54]. We can also expand this natural SUSY BM point into a natural SUSY model line by simply varying the A_0 parameter which results in variation of $m_{\tilde{t}_1}$: 800–2200 GeV while hardly changing m_h or other sparticle masses.

V. REACH OF LHC FOR NATURAL TOP SQUARKS

We next examine the reach of HL-LHC ($\sqrt{s} = 14$ TeV with 3000 fb^{-1}) for the top squarks of stringy natural SUSY. To proceed, we generate a SUSY Les Houches Accord file [72] for each of our natural SUSY model line points and feed this into PYTHIA [73], which is used for signal and the $2 \to 2$

BG processes. The $pp \to \tilde{t}_1\tilde{t}_1^* X$ cross section is normalized to the default Prospino NLO value from Fig. 8.

For the $2 \to 3$ BG processes, we use MadGraph [74] coupled to PYTHIA. The SM BGs considered are $t\bar{t}$, $b\bar{b}Z$, $t\bar{t}Z$, $t\bar{t}W$, $b\bar{b}W$, and single-top production. We evaluate all background processes using leading order PYTHIA and MadGraph results but normalize the total cross sections to the higher order perturbative results listed below:

(1) $t\bar{t}$: NNLO + NNLL result from Top + +v2.0 [75],
(2) $t\bar{t}W$ and $t\bar{t}Z$: NLO (QCD + EW) from Table 41 of [76],
(3) single top: NNLO result from [77],
(4) $Wb\bar{b}$ and $Zb\bar{b}$: NLO results from Table 6 of [78] extrapolated to $\sqrt{s} = 14$ TeV.

We adopt the toy detector simulation Delphes [79].

The baseline reconstructed objects are as follows.

Baseline small radius jet:

(1) Found by anti-k_t jet finder algorithm with $p_T(\text{min}) = 25$ GeV and $R = 0.4$ and
(2) $|\eta(j)| < 4.5$.

Isolated lepton:

(1) $|\eta(\mu)| < 2.5$ for muon, $|\eta(e)| < 2.47$ for electron,
(2) $p_T(\mu) > 25$ GeV for muon, $p_T(e) > 20$ GeV for electron.

Large radius jet:

(1) Found by Cambridge/Aachen finder algorithm with $p_T(\text{min}) = 400$ GeV with $R = 1.5$.

For signal objects, we also require signal b jets:

(1) satisfy the baseline small radius jet requirement above,
(2) $|\eta(b)| < 2.4$, and
(3) tagged by Delphes as b jet. [The b-jet tagging efficiency for our $p_T(b)$ range occurs at around the 75% level from Delphes.]

The signal top candidate is reconstructed with either of the following criteria:

(1) The fat jet J is tagged by the HEPTopTagger2 [80,81] as a top. In such case, the top four-vector reconstructed by the tagger is used for further kinematics calculations, or
(2) The fat jet J has a trimmed mass 115 GeV $< m_J <$ 225 GeV and has at least $1b$ jet within the cone radius of the fat jet [$\Delta R(J, b) < 1.5$]. In such a case, the trimmed four-vector of the fat jet is used for further kinematics calculations.

(Using this procedure, we compute the single top-jet tag efficiency as about 71% for a single top-jet; but this drops to ~36% for events containing two top jets.)

The events then are separated into three channels: $t\bar{t} + \not{E}_T$, $tb + \not{E}_T$, and $b\bar{b} + \not{E}_T$. For each signal channel, we veto events containing isolated leptons. The workflow to determine each channel is as follows:

(1) If there are at least two tops being tagged by the HEPTopTagger2, the two tops with the hardest p_T are chosen as signals, and this channel is labeled as $t\bar{t} + \not{E}_T$.
(2) Otherwise, if the HEPTopTagger2 tags 1 top, and the trimming method tags at least one other, this channel is labeled again as $t\bar{t} + \not{E}_T$. The top tagged by the HEPTopTagger2, and the hardest fat jet found by the trimming method are chosen as signals.
(3) Otherwise, if the HEPTopTagger2 fails to tag any tops, but the trimming method found at least two, this channel is also labeled as $t\bar{t} + \not{E}_T$. The two tops with the hardest p_T are chosen as signals.
(4) Otherwise, if there is exactly 1 top tagged by either HEPTopTagger2 or the trimming method, then look for extra b-jet candidates. The b-jet candidates must satisfy signal b-jet requirement listed above. The b-jet candidate needs to be well separated with the three subjets of the reconstructed top (both HEPTopTagger2 and the trimming algorithm can provide the subjet four-vectors): $\Delta R(\text{subjet}, b) > 0.4$. If there are b jets satisfying these requirements, then the b candidate that minimizes the vector sum of $\not{E}_T + p_T(t) + p_T(b)$ is chosen as the signal. This channel is labeled as $tb + \not{E}_T$.
(5) Otherwise, if the event fails any of the above selection requirements but has at least two b jets satisfied the signal b-jet requirement, this channel is labeled as $b\bar{b} + \not{E}_T$. The pair of b jets that minimize the vector sum of $\not{E}_T + p_T(b_1) + p_T(b_2)$ are chosen as signals. The harder of the two is labeled as b_1, and the other is b_2 in the following.

A. $b\bar{b} + \not{E}_T$

We first examine the $b\bar{b} + \not{E}_T$ channel. After examining various distributions, we require the following:

(1) $\not{E}_T > 800$ GeV,
(2) $|\eta(b_1)| < 2.0$,
(3) $p_T(b_1) > 200$ GeV,
(4) $H_T > 1500$ GeV,
(5) $\min[m_T(b_1, \not{E}_T), m_T(b_2, \not{E}_T)] > 175$ GeV,
(6) $\min(\Delta\phi(b, \not{E}_T)) > 20°$, where b loops over all b jets in the event.

After these cuts, we construct the m_{T2} distribution [82] and plot the resultant distribution in Fig. 10. The strategy becomes clear: look for a high m_{T2} deviation from expected background at the higher m_{T2} values where we expect m_{T2} to be bounded from above by $m_{\tilde{t}_1}$. In the plot, we show signal histograms for five different values of $m_{\tilde{t}_1}$ along with leading backgrounds. While BG does indeed dominate at low m_{T2}, a signal emerges from BG at higher values. If there are sufficient number of signal events above BG, then a signal can be claimed.

B. $tb + \not{E}_T$

After examining various distributions, for the $tb + \not{E}_T$ channel we require

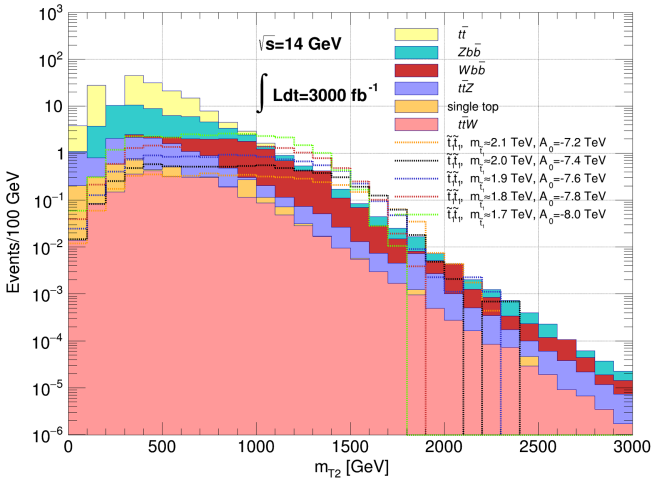

FIG. 10. Distribution in m_{T2} from top-squark pair production at LHC14 in the $b\bar{b}+\not{E}_T$ channel along with dominant SM backgrounds after cuts listed in the text.

(1) $\not{E}_T > 400$ GeV,
(2) $H_T > 1400$ GeV,
(3) $L_T > 1800$ GeV [defined as the scalar sum of $p_T(t) + p_T(b) + \not{E}_T$], where t and b here are the signal top and b jet,
(4) $\min[m_T(t, \not{E}_T), m_T(b, \not{E}_T)] > 175$ GeV,
(5) $\min(\Delta\phi(b, \not{E}_T)) > 40°$, where b loops over all b jets in the event,
(6) $\min(\Delta\phi(J, \not{E}_T)) > 30°$, where J loops over all fat jets in the event, no matter whether they have been tagged as top or not.

The resultant m_{T2} distribution is shown in Fig. 11 where again we expect the signal distribution to be bounded from above by $m_{\tilde{t}_1}$ whilst BG is a continuum. The five signal histograms do indeed emerge from BG at high m_{T2} although not necessarily at an observable rate. The largest BG at high m_{T2} is from $t\bar{t}Z$ production.

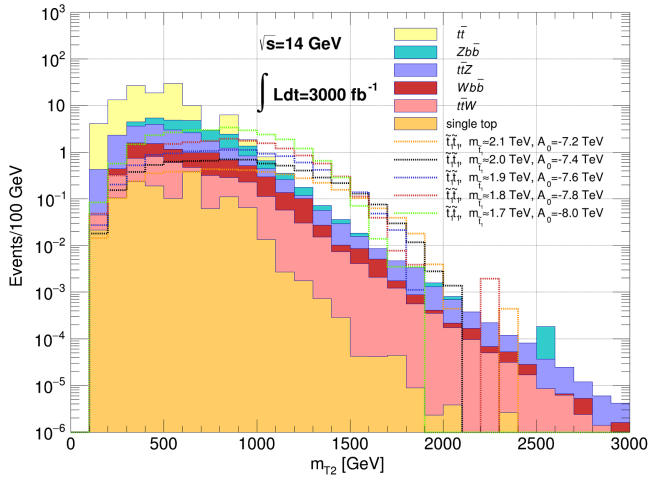

FIG. 11. Distribution in m_{T2} from top-squark pair production at LHC14 in the $tb+\not{E}_T$ channel along with dominant SM backgrounds after cuts listed in the text.

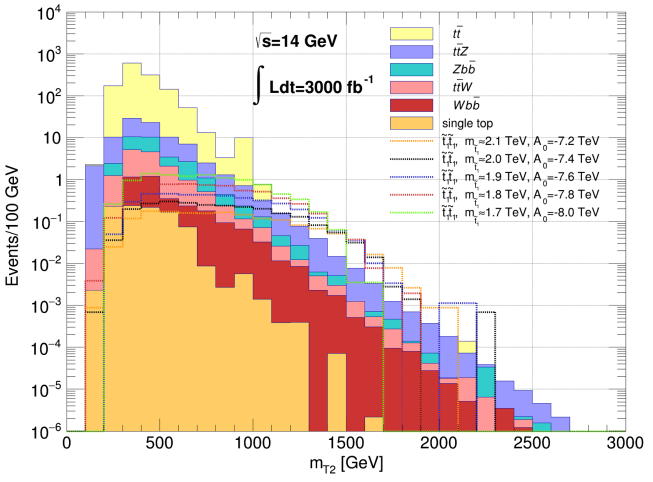

FIG. 12. Distribution in m_{T2} from top-squark pair production at LHC14 in the $t\bar{t}+\not{E}_T$ channel along with dominant SM backgrounds after cuts listed in the text.

C. $t\bar{t}+\not{E}_T$

Next, we examine various distributions for signal and BG in the $t\bar{t}+\not{E}_T$ signal channel. We then require the following:

(1) $\not{E}_T > 300$ GeV,
(2) $H_T > 1400$ GeV,
(3) $\min[m_T(t_1, \not{E}_T), m_T(t_2, \not{E}_T)] > 175$ GeV,
(4) $\min(\Delta\phi(b, \not{E}_T)) > 40°$, where b loops over all b jets in the event,
(5) $\min(\Delta\phi(J, \not{E}_T)) > 30°$, where J loops over all fat jets in the event, no matter whether they have been tagged as top or not.

The subsequent m_{T2} distribution is plotted in Fig. 12. The signal distributions emerge from SM BG at high m_{T2} but at more marginal rates than the other channels due to the lower efficiency to tag top jets.

D. Cumulative reach of HL-LHC for top squark pair production in natSUSY

Using the analysis cuts for the various signal channels discussed above, we can now create reach plots to show the HL-LHC discovery sensitivity versus $m_{\tilde{t}_1}$ along our natural SUSY model line. We use the 5σ level to claim discovery of a top squark and assume the true distribution one observes experimentally corresponds to signal plus background. For the signal, we fold in the approximate $\pm(15-35)\%$ theory uncertainty from the Prospino total cross sections for $pp \to \tilde{t}_1\tilde{t}_1^* X$ production.[4] In Fig. 13, we assume no systematic error while in Fig. 14 we add in a systematic error affecting background yields for each m_{T2} bin of 25% times the statistical error. We then test this against the background-only distribution in order to see if the background-only hypothesis can be rejected at the 5σ level. Specifically, compute the product of likelihoods from each bin of the

[4]See https://twiki.cern.ch/twiki/bin/view/LHCPhysics/SUSYCrossSections14TeVstopsbottom.

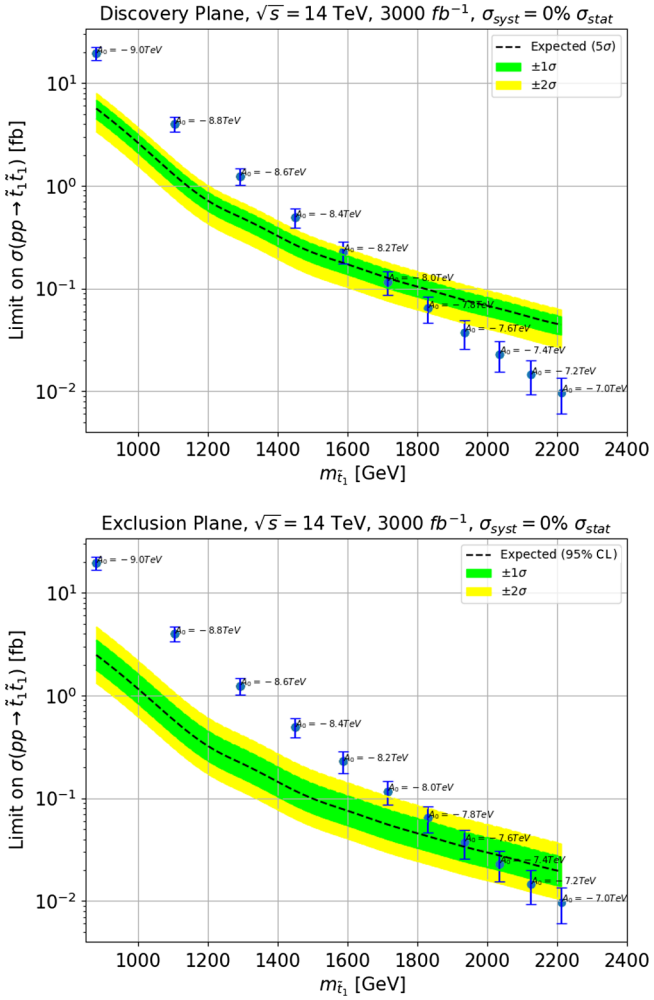

FIG. 13. Expected 5σ discovery limit and expected 95% CL exclusion limit on top-squark pair production cross section vs $m_{\tilde{t}_1}$ from a natural SUSY model line at HL-LHC with $\sqrt{s} = 14$ TeV and 3000 fb^{-1} of integrated luminosity.

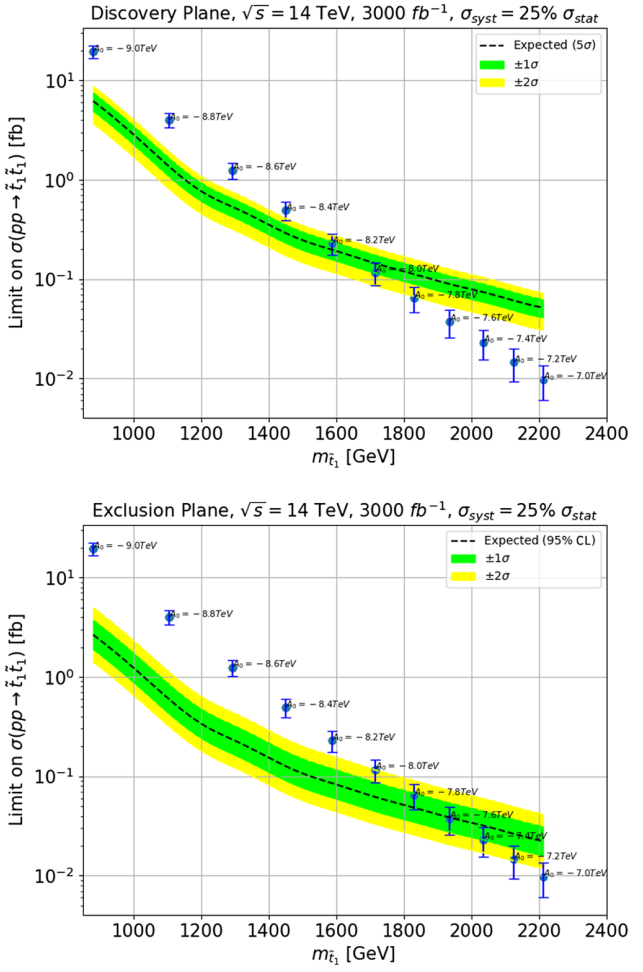

FIG. 14. Expected 5σ discovery limit and expected 95% CL exclusion limit on top-squark pair production cross section vs $m_{\tilde{t}_1}$ from a natural SUSY model line at HL-LHC with $\sqrt{s} = 14$ TeV and 3000 fb^{-1} of integrated luminosity with 25% systematic errors folded in.

entire m_{T2} distributions (bin width of 100 GeV) and from each signal channel as displayed above to obtain the discovery/exclusion limits.[5]

In the case of the exclusion line, the upper limits for exclusion of a signal are set at 95% CL; one assumes the true distribution one observes in experiment corresponds to background only. The limits are then computed using a modified frequentist CL_s method [84] where the profile likelihood ratio is the test statistic. For both the exclusion and discovery plots, the asymptotic approximation for obtaining the median significance is employed [85]. For both discovery and exclusion estimates, we combine results from all three top-squark signal channels: $t\bar{t} + \not{E}_T$, $b\bar{b} + \not{E}_T$, and $tb + \not{E}_T$.

As an example of the remaining signal and background after cuts (for 3000 fb^{-1} of integrated luminosity) for each signal channel, and for $m_{T2} > 900$ GeV, we list in Table II the number of remaining events for background and for several signal benchmarks.[6] The hard cuts

[5]For the profile likelihood in more detail, the likelihood L is built as the product of Poissonian terms for each of the bins in the m_{T2} plots. The background systematic is introduced with an independent nuisance parameter for each bin (following Ref. [47]) and the likelihood is modified by log-normal terms to account for these nuisance parameters, with an assumed systematic uncertainty equal to 25% statistical uncertainty. (From Ref. [83], both Gaussian and log-normal distributions on the constraint term are common choices. We used the log-normal to avoid negative background yield, which in the Gaussian case could possibly happen.) These nuisance parameters are then fitted with the likelihood function for each of the bins. We treat the Monte Carlo simulation directly as the pseudoexperiment results that one would observe. We do not include in our reach determination any variation in the NLO top squark pair production, which amounts to about 15–35% overall uncertainty. But this deviation can be read off from the signal error bars. The 1σ and 2σ bands in our reach plots are purely statistical for Fig. 13 and combined statistical/systematic for Fig. 14.

[6]Table II is for illustration only; in our actual analysis, all m_{T2} bins are used for the likelihood calculations and no specific m_{T2} cut is used.

TABLE II. Number of events left per 3000 fb^{-1} after cuts for each signal channel and with $m_{T2} > 900$ GeV.

Channel	$1b1t$	bb	tt
Background	9.1	18.3	13.0
BM($m_{\tilde{t}_1} = 1714$ GeV)	9.4	10.1	2.8
BM($m_{\tilde{t}_1} = 1830$ GeV)	6.4	6.8	1.9
BM($m_{\tilde{t}_1} = 1935$ GeV)	4.4	4.5	1.4
BM($m_{\tilde{t}_1} = 2034$ GeV)	2.9	3.1	0.9
BM($m_{\tilde{t}_1} = 2126$ GeV)	2.0	2.1	0.6

we impose generally reduce the remaining events to a minimal level required to be able to claim a signal or an exclusion.[7]

In Fig. 13(a), we show the 5σ discovery cross section as the dashed line along with 1- and 2-σ error bands. We show the corresponding natural SUSY model line as blue dots with error bars corresponding to the overall uncertainty on the NLO production cross section. We see that HL-LHC with 3000 fb^{-1} of integrated luminosity can discover natural SUSY top squarks out to $m_{\tilde{t}_1} \sim 1.65$ TeV. In Fig. 13(b), we plot the HL-LHC 95% exclusion reach. In this case, the exclusion reach extends out to $m_{\tilde{t}_1} \sim 1.95$ TeV. By folding in the statistical uncertainty from the 1σ and 2σ bands, we can modify our central results of a stop discovery reach to $m_{\tilde{t}_1} \sim 1.6$–1.8 TeV (1σ) and $m_{\tilde{t}_1} \sim 1.55$–$1.9$ TeV (2σ). Similarly, the 95% CL exclusion reach is modified to $m_{\tilde{t}_1} \sim 1.85$–$2.1$ TeV (1σ) and $m_{\tilde{t}_1} \sim 1.7$–2.2 TeV (2σ). By comparing our central results with expectations from stringy naturalness in Fig. 1(b), we see that HL-LHC can cover the bulk of stringy natural parameter space, although a tail of probability where HL-LHC would not discover top squarks does extend past $m_{\tilde{t}_1} \sim 2$ TeV.

In Fig. 14, we show again the discovery reach and 95% CL exclusion plots but this time folding in an assumed systematic error of 25% times the statistical error for each m_{T2} bin.[8] In this case, the reach is somewhat reduced: for instance, the discovery reach for 3000 fb^{-1} is reduced from about $m_{\tilde{t}_1} \sim 1.65$ TeV with no systematic error to about 1.6 TeV including the systematic errors.

[7]In Figs. 10–12, our dominant backgrounds at high m_{T2} are found to be $Zb\bar{b}$ and $Zt\bar{t}$. In the ATLAS analysis of HL-LHC reach for top squark pairs, their analysis, which is very different from ours and assumes 100% $\tilde{t} \to t\tilde{\chi}_1^0$ decay, tends to find a dominant single-top background for the highest p_T events.

[8]This is in rough accord with estimates from a similar ATLAS study: see Tables 9 and 10 of Ref. [7].

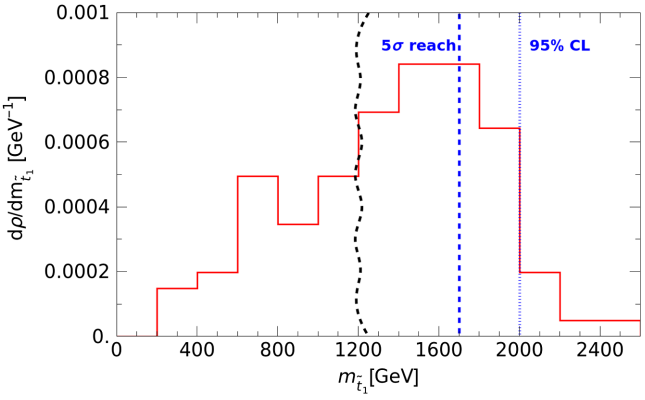

FIG. 15. Probability distribution for lighter top squark mass $m_{\tilde{t}_1}$ with an $n = 1$ power-law draw to large soft terms. We also show the present reach on $m_{\tilde{t}_1}$ from LHC run 2, and the expected HL-LHC 5σ and 95% CL reach.

VI. CONCLUSIONS

In this paper we have examined what sort of values of top squark masses and other properties are expected from the string landscape where a power-law draw to large soft terms is expected, but where the derived value of the weak scale must lie within the ABDS window in order to allow for complex nuclei (and hence atoms) in each anthropically allowed pocket universe. Under this stringy naturalness requirement, we find $m_{\tilde{t}_1} \sim 1$–2.5 TeV with large mixing. These results are in accord with measurements of BR($b \to s\gamma$) which are suggestive of TeV-scale top squarks so that SUSY contributions to this decay rate decouple. The large mixing helps boost $m_h \to 125$ GeV while minimizing the top squark contributions to the weak scale $\Sigma_u^u(\tilde{t}_{1,2})$.

In spite of the large mixing, the lighter top squark is mainly a right squark, but decays at $\tilde{t}_1 \to b\tilde{\chi}_1^+$ at ~50% and $\tilde{t}_1 \to t\tilde{\chi}_{1,2}^0$ at ~25% each. Thus, we expect top-squark pair production at LHC run 3 and HL-LHC to lead to mixed final states of $b\bar{b} + \not{E}_T$, $t\bar{t} + \not{E}_T$, and $tb + \not{E}_T$. We evaluated some optimized cuts for each of these channels, and then expect the top-squark pair production to be revealed as an enhancement in the m_{T2} distribution at high values of m_{T2}. We combined the reaches in these three channels to find that HL-LHC operating at $\sqrt{s} = 14$ TeV with 3000 fb^{-1} of integrated luminosity should have a 5σ discovery reach to $m_{\tilde{t}_1} \sim 1.65$ TeV and a 95% CL exclusion reach to about $m_{\tilde{t}_1} \sim 1.95$ TeV.[9]

[9]We may compare our HL-LHC reach for top squarks to the ATLAS analysis of Ref. [47] where they find a 5σ discovery (95% CL exclusion) reach to $m_{\tilde{t}_1} \sim 1.25(1.7)$ TeV. A large part of our improvement over the ATLAS result comes from our use of a (more plausible) natural SUSY model where the best discovery channels arise from the $\tilde{t}_1 \to b\tilde{\chi}_1^+$ decay mode which is not allowed in the simplified model assumed by ATLAS.

Now our HL-LHC reach results can be added to Fig. 1(b) as a final summary frame: Fig. 15. These HL-LHC reach limits will cover most (but not all) of the expected stringy natural parameter space from SUSY on the landscape!

ACKNOWLEDGMENTS

This material is based upon work supported by the U.S. Department of Energy, Office of Science, Office of High Energy Physics under Awards No. DE-SC-0009956 and No. DE-SC-0017647.

[1] J. R. Ellis, K. Enqvist, D. V. Nanopoulos, and F. Zwirner, Observables in low-energy superstring models, Mod. Phys. Lett. A **01**, 57 (1986).
[2] R. Barbieri and G. F. Giudice, Upper bounds on supersymmetric particle masses, Nucl. Phys. **B306**, 63 (1988).
[3] S. Dimopoulos and G. F. Giudice, Naturalness constraints in supersymmetric theories with nonuniversal soft terms, Phys. Lett. B **357**, 573 (1995).
[4] R. Kitano and Y. Nomura, Supersymmetry, naturalness, and signatures at the LHC, Phys. Rev. D **73**, 095004 (2006).
[5] M. Papucci, J. T. Ruderman, and A. Weiler, Natural SUSY endures, J. High Energy Phys. 09 (2012) 035.
[6] C. Brust, A. Katz, S. Lawrence, and R. Sundrum, SUSY, the third generation and the LHC, J. High Energy Phys. 03 (2012) 103.
[7] G. Aad *et al.*, Search for a scalar partner of the top quark in the all-hadronic $t\bar{t}$ plus missing transverse momentum final state at $\sqrt{s} = 13$ TeV with the ATLAS detector, Eur. Phys. J. C **80**, 737 (2020).
[8] G. Aad *et al.*, Search for new phenomena with top quark pairs in final states with one lepton, jets, and missing transverse momentum in pp collisions at $\sqrt{s} = 13$ TeV with the ATLAS detector, J. High Energy Phys. 04 (2021) 174.
[9] A. M. Sirunyan *et al.*, Search for top squark production in fully-hadronic final states in proton-proton collisions at $\sqrt{s} = 13$ TeV, Phys. Rev. D **104**, 052001 (2021).
[10] H. Baer and X. Tata, *Weak Scale Supersymmetry: From Superfields to Scattering Events* (Cambridge University Press, Cambridge, England, 2006).
[11] M. Dine, Naturalness under stress, Annu. Rev. Nucl. Part. Sci. **65**, 43 (2015).
[12] H. Baer, V. Barger, and D. Mickelson, How conventional measures overestimate electroweak fine-tuning in supersymmetric theory, Phys. Rev. D **88**, 095013 (2013).
[13] H. Baer, V. Barger, D. Martinez, and S. Salam, On practical naturalness and its implications for weak scale supersymmetry, Phys. Rev. D **108**, 035050 (2023).
[14] A. Mustafayev and X. Tata, Supersymmetry, naturalness, and light higgsinos, Indian J. Phys. **88**, 991 (2014).
[15] H. Baer, V. Barger, D. Mickelson, and M. Padeffke-Kirkland, SUSY models under siege: LHC constraints and electroweak fine-tuning, Phys. Rev. D **89**, 115019 (2014).
[16] A. Brignole, L. E. Ibanez, and C. Munoz, Towards a theory of soft terms for the supersymmetric standard model, Nucl. Phys. **B422**, 125 (1994); **B436**, 747(E) (1995).
[17] H. Baer, V. Barger, P. Huang, A. Mustafayev, and X. Tata, Radiative natural SUSY with a 125 GeV Higgs boson, Phys. Rev. Lett. **109**, 161802 (2012).
[18] H. Baer, V. Barger, P. Huang, D. Mickelson, A. Mustafayev, and X. Tata, Radiative natural supersymmetry: Reconciling electroweak fine-tuning and the Higgs boson mass, Phys. Rev. D **87**, 115028 (2013).
[19] H. Baer, V. Barger, S. Salam, D. Sengupta, and K. Sinha, Status of weak scale supersymmetry after LHC Run 2 and ton-scale noble liquid WIMP searches, Eur. Phys. J. Spec. Top. **229**, 3085 (2020).
[20] R. Bousso and J. Polchinski, The string theory landscape, Sci. Am. **291**, 60 (2004).
[21] L. Susskind, The anthropic landscape of string theory, arXiv:hep-th/0302219.
[22] M. R. Douglas and S. Kachru, Flux compactification, Rev. Mod. Phys. **79**, 733 (2007).
[23] S. Ashok and M. R. Douglas, Counting flux vacua, J. High Energy Phys. 01 (2004) 060.
[24] S. Weinberg, Anthropic bound on the cosmological constant, Phys. Rev. Lett. **59**, 2607 (1987).
[25] M. R. Douglas, Statistical analysis of the supersymmetry breaking scale, arXiv:hep-th/0405279.
[26] V. Agrawal, S. M. Barr, J. F. Donoghue, and D. Seckel, Viable range of the mass scale of the standard model, Phys. Rev. D **57**, 5480 (1998).
[27] H. Baer, V. Barger, H. Serce, and K. Sinha, Higgs and superparticle mass predictions from the landscape, J. High Energy Phys. 03 (2018) 002.
[28] S. K. Soni and H. A. Weldon, Analysis of the supersymmetry breaking induced by $N = 1$ supergravity theories, Phys. Lett. **126B**, 215 (1983).
[29] V. S. Kaplunovsky and J. Louis, Model independent analysis of soft terms in effective supergravity and in string theory, Phys. Lett. B **306**, 269 (1993).
[30] H. Baer, V. Barger, and D. Sengupta, Landscape solution to the SUSY flavor and *CP* problems, Phys. Rev. Res. **1**, 033179 (2019).
[31] H. Baer, V. Barger, and P. Huang, Hidden SUSY at the LHC: The light Higgsino-world scenario and the role of a lepton collider, J. High Energy Phys. 11 (2011) 031.
[32] Z. Han, G. D. Kribs, A. Martin, and A. Menon, Hunting quasidegenerate higgsinos, Phys. Rev. D **89**, 075007 (2014).
[33] H. Baer, A. Mustafayev, and X. Tata, Monojet plus soft dilepton signal from light higgsino pair production at LHC14, Phys. Rev. D **90**, 115007 (2014).

[34] C. Han, D. Kim, S. Munir, and M. Park, Accessing the core of naturalness, nearly degenerate higgsinos, at the LHC, J. High Energy Phys. 04 (2015) 132.

[35] H. Baer, V. Barger, S. Salam, D. Sengupta, and X. Tata, The LHC higgsino discovery plane for present and future SUSY searches, Phys. Lett. B **810**, 135777 (2020).

[36] H. Baer, V. Barger, D. Sengupta, and X. Tata, New angular and other cuts to improve the Higgsino signal at the LHC, Phys. Rev. D **105**, 095017 (2022).

[37] I. I. Y. Bigi and S. Rudaz, Search for scalar superpartners of the top quark, Phys. Lett. **153B**, 335 (1985).

[38] H. Baer and X. Tata, Implications of the T quark signal for stop squarks and charged Higgs bosons, Phys. Lett. **167B**, 241 (1986).

[39] H. Baer, M. Drees, R. Godbole, J. F. Gunion, and X. Tata, Phenomenology of light top squarks at the Fermilab Tevatron, Phys. Rev. D **44**, 725 (1991).

[40] H. Baer, J. Sender, and X. Tata, The search for top squarks at the Fermilab tevatron collider, Phys. Rev. D **50**, 4517 (1994).

[41] K. Rolbiecki, J. Tattersall, and G. Moortgat-Pick, Towards measuring the stop mixing angle at the LHC, Eur. Phys. J. C **71**, 1517 (2011).

[42] F. Brummer, S. Kraml, and S. Kulkarni, Anatomy of maximal stop mixing in the MSSM, J. High Energy Phys. 08 (2012) 089.

[43] M. L. Graesser and J. Shelton, Hunting mixed top squark decays, Phys. Rev. Lett. **111**, 121802 (2013).

[44] H. Baer, V. Barger, N. Nagata, and M. Savoy, Phenomenological profile of top squarks from natural supersymmetry at the LHC, Phys. Rev. D **95**, 055012 (2017).

[45] C. Han, J. Ren, L. Wu, J. M. Yang, and M. Zhang, Top-squark in natural SUSY under current LHC run-2 data, Eur. Phys. J. C **77**, 93 (2017).

[46] Y. Bai, J. Berger, J. Osborne, and B. A. Stefanek, Search for heavy stops with merged top-jets, Phys. Rev. D **96**, 095035 (2017).

[47] ATLAS Collaboration, ATLAS sensitivity to top squark pair production at the HL-LHC, Report No. ATL-PHYS-PUB-2018-021, 2018.

[48] X. Cid Vidal *et al.*, Report from working group 3: Beyond the standard model physics at the HL-LHC and HE-LHC, CERN Yellow Rep. Monogr. **7**, 585 (2019).

[49] H. Baer, V. Barger, S. Salam, and D. Sengupta, String landscape guide to soft SUSY breaking terms, Phys. Rev. D **102**, 075012 (2020).

[50] M. R. Douglas, *The String Landscape and Low Energy Supersymmetry* (World Scientific, Singapore, 2012), pp. 261–288, 10.1142/9789814412551_0012.

[51] H. Baer, V. Barger, and S. Salam, Naturalness versus stringy naturalness (with implications for collider and dark matter searches), Phys. Rev. Res. **1**, 023001 (2019).

[52] H. Baer, A. Mustafayev, S. Profumo, A. Belyaev, and X. Tata, Direct, indirect and collider detection of neutralino dark matter in SUSY models with non-universal Higgs masses, J. High Energy Phys. 07 (2005) 065.

[53] K. J. Bae, H. Baer, V. Barger, and D. Sengupta, Revisiting the SUSY μ problem and its solutions in the LHC era, Phys. Rev. D **99**, 115027 (2019).

[54] F. E. Paige, S. D. Protopopescu, H. Baer, and X. Tata, ISAJET 7.69: A Monte Carlo event generator for pp, anti-p p, and $e+e-$ reactions, arXiv:hep-ph/0312045.

[55] M. Carena and H. E. Haber, Higgs boson theory and phenomenology, Prog. Part. Nucl. Phys. **50**, 63 (2003).

[56] H. Baer, V. Barger, and A. Mustafayev, Implications of a 125 GeV Higgs scalar for LHC SUSY and neutralino dark matter searches, Phys. Rev. D **85**, 075010 (2012).

[57] V. Barger, P. Huang, M. Ishida, and W.-Y. Keung, Scalar-top masses from SUSY loops with 125 GeV mh and precise Mw, Phys. Lett. B **718**, 1024 (2013).

[58] V. D. Barger, J. L. Hewett, and R. J. N. Phillips, New constraints on the charged Higgs sector in two Higgs doublet models, Phys. Rev. D **41**, 3421 (1990).

[59] H. Baer and M. Brhlik, QCD improved $b \to s\gamma$ constraints on the minimal supergravity model, Phys. Rev. D **55**, 3201 (1997).

[60] H. Baer, M. Brhlik, D. Castano, and X. Tata, $b \to s\gamma$ constraints on the minimal supergravity model with large tan Beta, Phys. Rev. D **58**, 015007 (1998).

[61] M. Misiak, Radiative decays of the B meson: A progress report, Acta Phys. Pol. B **49**, 1291 (2018).

[62] Y. Amhis *et al.*, Averages of b-hadron, c-hadron, and τ-lepton properties as of 2021, Phys. Rev. D **107**, 052008 (2023).

[63] A. Limosani *et al.*, Measurement of inclusive radiative B-meson decays with a photon energy threshold of 1.7-GeV, Phys. Rev. Lett. **103**, 241801 (2009).

[64] J. P. Lees *et al.*, Precision measurement of the $B \to X_s\gamma$ photon energy spectrum, branching fraction, and direct CP asymmetry $A_{CP}(B \to X_{s+d}\gamma)$, Phys. Rev. Lett. **109**, 191801 (2012).

[65] W. Beenakker, R. Hopker, and M. Spira, PROSPINO: A program for the production of supersymmetric particles in next-to-leading order QCD, arXiv:hep-ph/9611232.

[66] G. Aad *et al.*, Search for charginos and neutralinos in final states with two boosted hadronically decaying bosons and missing transverse momentum in pp collisions at $\sqrt{s} =$ 13 TeV with the ATLAS detector, Phys. Rev. D **104**, 112010 (2021).

[67] S. Kraml, S. Kulkarni, U. Laa, A. Lessa, W. Magerl, D. Proschofsky-Spindler, and W. Waltenberger, SModelS: A tool for interpreting simplified-model results from the LHC and its application to supersymmetry, Eur. Phys. J. C **74**, 2868 (2014).

[68] G. Alguero, J. Heisig, C. K. Khosa, S. Kraml, S. Kulkarni, A. Lessa, H. Reyes-González, W. Waltenberger, and A. Wongel, Constraining new physics with SModelS version 2, J. High Energy Phys. 08 (2022) 068.

[69] M. Drees, H. Dreiner, D. Schmeier, J. Tattersall, and J. S. Kim, CheckMATE: Confronting your favourite new physics model with LHC data, Comput. Phys. Commun. **187**, 227 (2015).

[70] D. Dercks, N. Desai, J. S. Kim, K. Rolbiecki, J. Tattersall, and T. Weber, CheckMATE2: From the model to the limit, Comput. Phys. Commun. **221**, 383 (2017).

[71] H. Baer, C.-H. Chen, R. B. Munroe, F. E. Paige, and X. Tata, Multichannel search for minimal supergravity at $p\bar{p}$ and e^+e^- colliders, Phys. Rev. D **51**, 1046 (1995).

[72] P. Z. Skands *et al.*, SUSY Les Houches accord: Interfacing SUSY spectrum calculators, decay packages, and event generators, J. High Energy Phys. 07 (2004) 036.
[73] T. Sjostrand, S. Mrenna, and P. Z. Skands, PYTHIA6.4 physics and manual, J. High Energy Phys. 05 (2006) 026.
[74] J. Alwall, M. Herquet, F. Maltoni, O. Mattelaer, and T. Stelzer, MadGraph5: Going beyond, J. High Energy Phys. 06 (2011) 128.
[75] M. Czakon and A. Mitov, Top + +: A program for the calculation of the top-pair cross-section at hadron colliders, Comput. Phys. Commun. **185**, 2930 (2014).
[76] D. de Florian *et al.*, Handbook of LHC Higgs cross sections: 4. Deciphering the nature of the Higgs sector, arXiv:1610.07922.
[77] N. Kidonakis, Theoretical results for electroweak-boson and single-top production, Proc. Sci., DIS2015 (**2015**) 170 [arXiv:1506.04072].
[78] J. Alwall, R. Frederix, S. Frixione, V. Hirschi, F. Maltoni, O. Mattelaer, H. S. Shao, T. Stelzer, P. Torrielli, and M. Zaro, The automated computation of tree-level and next-to-leading order differential cross sections, and their matching to parton shower simulations, J. High Energy Phys. 07 (2014) 079.
[79] J. de Favereau, C. Delaere, P. Demin, A. Giammanco, V. Lemaître, A. Mertens, and M. Selvaggi, DELPHES 3, A modular framework for fast simulation of a generic collider experiment, J. High Energy Phys. 02 (2014) 057.
[80] C. Anders, C. Bernaciak, G. Kasieczka, T. Plehn, and T. Schell, Benchmarking an even better top tagger algorithm, Phys. Rev. D **89**, 074047 (2014).
[81] T. Plehn, M. Spannowsky, and M. Takeuchi, How to improve top tagging, Phys. Rev. D **85**, 034029 (2012).
[82] A. Barr, C. Lester, and P. Stephens, m(T2): The truth behind the glamour, J. Phys. G **29**, 2343 (2003).
[83] L. Lista, Practical statistics for particle physicists, in *Proceedings of the 2016 European School of High-Energy Physics* (CERN Yellow Reports, Geneva, 2017), pp. 213–258, arXiv:1609.04150.
[84] A. L. Read, Presentation of search results: The CL_s technique, J. Phys. G **28**, 2693 (2002).
[85] G. Cowan, K. Cranmer, E. Gross, and O. Vitells, Asymptotic formulae for likelihood-based tests of new physics, Eur. Phys. J. C **71**, 1554 (2011).